A model for calculating impact ionization transition rate in wurtzite GaN for use in breakdown voltage simulation

Kazuki Kodama, Hirokuni Tokuda, and Masaaki Kuzuhara

Citation: Journal of Applied Physics **114**, 044509 (2013); doi: 10.1063/1.4817028
View online: http://dx.doi.org/10.1063/1.4817028
View Table of Contents: http://scitation.aip.org/content/aip/journal/jap/114/4?ver=pdfcov
Published by the AIP Publishing

A model for calculating impact ionization transition rate in wurtzite GaN for use in breakdown voltage simulation

Kazuki Kodama, Hirokuni Tokuda, and Masaaki Kuzuhara
Graduate School of Engineering, University of Fukui, 3-9-1 Bunkyo, Fukui 910-8507, Japan

(Received 9 April 2013; accepted 15 July 2013; published online 31 July 2013)

A model for calculating impact ionization transition rate (IITR) in wurtzite GaN has been developed for use in breakdown voltage simulations. The characteristic feature of the model is to calculate energy-dependent IITR by taking a conduction band index into account. Depending on the band index, the IITR values calculated by the proposed model show spreading by three orders of magnitude in the electron energy range from 6.5 to 8 eV, while this spreading is totally disregarded in the conventional model. An impact ionization coefficient is calculated based on a full band Monte Carlo simulation which incorporates IITRs by the proposed model. The calculated impact ionization coefficients by the proposed model exhibit better agreements with those by the rigorous model. The proposed model is applied to the calculation of breakdown characteristics for AlGaN/GaN HEMTs and demonstrates a higher breakdown voltage by about 30% than that by the conventional model. © *2013 AIP Publishing LLC*. [http://dx.doi.org/10.1063/1.4817028]

I. INTRODUCTION

Gallium nitride (GaN) is an attractive material for high-power[1–3] and high-frequency[4–6] device applications due to its inherent material properties, such as high peak electron velocity[7,8] ($>2.5\times10^7$ cm/s) and high breakdown electric field[9] ($\sim$3 MV/cm). It is known that an impact ionization coefficient of wurtzite GaN (Refs. 10 and 11) is about two orders of magnitude smaller than that of silicon.[12,13] Karmalkar and Mishra calculated breakdown characteristics for AlGaN/GaN HEMTs with a field plate structure based on the impact ionization coefficient.[14] However, inclusion of the impact ionization transition rate (IITR) is necessary to provide accurate theoretical accounting of the transport dynamics at high electric fields.[10]

For device simulations based on IITRs, an averaged IITR has been commonly used as a way of calculating breakdown characteristics. Ando *et al.* simulated breakdown characteristics in AlGaN/GaN HEMTs using the ionization model with simply averaged IITRs, in which the effect of conduction band index was ignored. They also reported a breakdown voltage (V_{br}) of 300 V for the device with a gate-to-drain distance (L_{gd}) of 1.8 μm,[15] corresponding to an averaged breakdown electric field, defined as V_{br}/L_{gd}, of 1.6 MV/cm. This value is comparable with those extracted experimentally using AlGaN/GaN HEMTs, i.e., 1–1.8 MV/cm.[16–20] Although further challenges for improving device performances have been done by taking sophisticated device structures such as double channel[21] and back barrier[22] HEMTs, these breakdown fields are still lower than the expected critical breakdown field for GaN ($\sim$3 MV/cm).

In this paper, a model for calculating IITR in wurtzite GaN is developed based on the improved approach taking the conduction band index into account. Impact ionization coefficients are calculated by the proposed model and the results are compared to reveal the importance of band index for initial electrons in calculating IITRs. The proposed model is used for the calculation of breakdown characteristics in AlGaN/GaN HEMTs based on a full band Monte Carlo device simulation.

II. MODEL DESCRIPTION

The band structure of wurtzite GaN was calculated based on an empirical pseudopotential method.[23,24] The pseudopotential consists of 19 form factors with non-zero values.[25] The reciprocal wave vectors of 147 were employed for Fourier series expansion of the wave function. An energy eigenvalue was calculated for 51 701 wave vector points in a 1/8 volume of the first Brillouin zone (BZ). Figure 1 shows the calculated band structure for wurtzite GaN with band indexes in conduction band (CB) and valence band (VB). Lowest six band indexes in CB and highest six indexes in VB were considered to cover electron energies up/down to $\pm$10 eV.

Figure 2(a) shows the calculated density of states (DOS) as a function of electron energy. A sharp increase in DOS was observed at electron energy of around 2 eV, reaching a peak of 5.2×10^{22} cm^{-3}eV^{-1} at 6.6 eV. The normalized DOS for each band index is shown in Fig. 2(b), where the normalized DOS at a given energy is defined as the DOS for each band index divided by the total DOS for all band indexes. As shown in Fig. 2(b), the peak of normalized DOS shifted toward higher electron energy with increasing the band index.

In the following, a calculation procedure of IITR is described for three models, i.e., rigorous, conventional, and proposed models.

(i) Rigorous model.
The rigorous IITR, W_{iir}, is calculated from Fermi's golden rule as[26,27]

$$W_{iir}(n_1,\boldsymbol{k}_1)=\frac{2\pi}{\hbar}\frac{V^2}{(2\pi)^6}\sum_{n_{1'},n_2,n_{2'}}\int d^3\boldsymbol{k}_{1'}\int d^3\boldsymbol{k}_{2'}\times|M|^2\,\delta(E_1+E_2-E_{1'}-E_{2'}),\qquad(1)$$

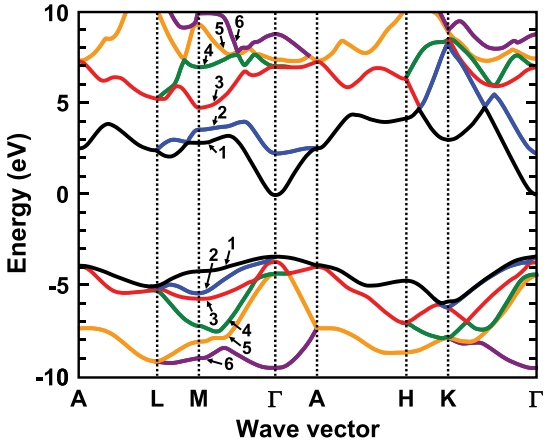

FIG. 1. Calculated band structure for wurtzite GaN along high symmetry line in 1st Brillouin zone. Numbers indicate band indexes.

where $\hbar$ is the Planck's constant divided by 2π, V is the crystal volume, M is the matrix element of Coulomb interaction, k_i is the electron wave vector, E_i is the electron energy, and n_i is the band index. The subscript i indicates the electron state. States 1 and 2 correspond to initial electron states in CB and VB, respectively, and states $1'$ and $2'$ are the corresponding final electron states in CB after transition. The state 1 was treated as an electron state located in the reduced region, which was 1/8 of the first BZ, while the other states (2, $1'$, and $2'$) were considered as electron states located in the entire first BZ. The matrix element M is given by[27]

$$M = \frac{1}{2}|M_D{}^2 + M_E{}^2 + (M_D - M_E)^2|, \tag{2a}$$

where M_D and M_E represent matrix elements of direct and exchange processes, respectively. M_D is expressed as

$$M_D = \frac{4\pi e^2}{V}\sum_G \times \frac{I_{cc}(n_1,\boldsymbol{k}_1;n_{1'},\boldsymbol{k}_{1'};\boldsymbol{G}) + I_{vc}(n_2,\boldsymbol{k}_2;n_{2'},\boldsymbol{k}_{2'};\boldsymbol{G})}{\varepsilon(\boldsymbol{q})(\boldsymbol{q}^2+\lambda^2)}, \tag{2b}$$

where I_{cc} is the overlap integral between states 1 and $1'$, I_{vc} is that between states 2 and $2'$, ε is the dielectric function,[28] e is the elementary charge, G is the reciprocal wave vector, q is the momentum transfer expressed as $k_1 + G_1 - k_{1'} - G_{1'}$, λ is the inverse of screening length. The M_E is calculated by simply exchanging two final electron states in CB as $(1', 2') \rightarrow (2', 1')$. The momentum conservation law includes umklapp process for calculating the matrix element. In the calculation, an electron carrier concentration of $1 \times 10^{17}\,\mathrm{cm}^{-3}$ and an absolute temperature of 300 K were assumed.

(ii) Conventional model.

The conventional IITR, W_{iic}, is expressed by simply averaging over transition rates based on the rigorous model for all initial electron states located in a given energy interval as[29–31]

$$W_{iic}(E) = \frac{\sum_{n_1}\int d^3\boldsymbol{k}_1\,\delta[E - E(n_1,\boldsymbol{k}_1)]W_{iir}(n_1,\boldsymbol{k}_1)}{\sum_{n_1}\int d^3\boldsymbol{k}_1\,\delta[E - E(n_1,\boldsymbol{k}_1)]}. \tag{3}$$

In Eq. (3), the delta function was calculated using the procedure reported by Kolnik *et al.*[29] An energy interval δE of 0.01 eV was assumed. The denominator in Eq. (3) corresponds to the total number of electron states belonging to energy interval between E and $E + \delta E$, while the numerator indicates the sum of IITRs belonging to the same energy interval of δE. Thus, Eq. (3) gives IITR averaged by the total number of electron states located in the energy interval. Although the conduction band index is included in the right side of Eq. (3), the summation over n_1 leads to the conventional IITR, which does not depend on the band index.

(iii) Proposed model.

The proposed IITR, W_{iip}, is expressed as

$$W_{iip}(n_1,E) = \frac{\int d^3\boldsymbol{k}_1\delta[E - E(n_1,\boldsymbol{k}_1)]W_{iir}(n_1,\boldsymbol{k}_1)}{\int d^3\boldsymbol{k}_1\delta[E - E(n_1,\boldsymbol{k}_1)]}. \tag{4}$$

The delta function in Eq. (4) was calculated using the same procedure as Eq. (3) with $\delta E = 0.01$ eV. Note

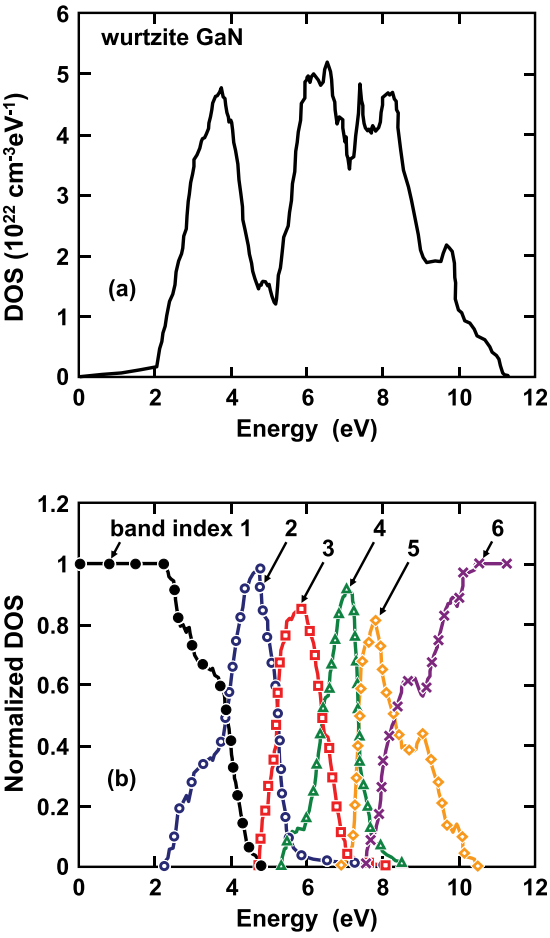

FIG. 2. (a) Calculated DOS in conduction band as a function of electron energy. (b) Normalized DOS for each band index as a function of electron energy. Each symbol corresponds to band index.

that the difference between Eqs. (3) and (4) lies in the treatment of summation function in terms of the initial band index. Total exclusion of summation over band index in Eq. (4) corresponds to averaging of rigorous IITRs at each band index, indicating that information on the initial band index is conserved in the proposed model. The proposed model gives an energy-dependent transition rate corresponding to each band index.

III. RESULTS AND DISCUSSION

Figure 3 shows calculated IITRs as a function of electron energy by the rigorous model. The threshold energy of IITR was around 3.8 eV, which was determined as the minimum electron energy to satisfy both energy and momentum conservations. It was higher than a band gap of 3.4 eV in GaN. Above 3.8 eV, IITRs showed spreading by 2–4 orders of magnitude. The spreading was attributed to the band index and the wave vector of initial electrons.

Figure 4 shows impact ionization processes for initial electrons in state 1 located at (a) Γ and (b) M points. Arrows by solid line show the probable electron transition path from states 1 to 1′ and the corresponding path from states 2 to 2′. Arrows by broken line show another transition path from states 1 to 1′ and the corresponding path from states 2 to 2′. Here, state 1′ in broken arrow is the symmetric point of state 1′ in the solid arrow. When the initial electron is located at Γ point (Fig. 4(a)), both transitions shown as solid and broken arrows are equally probable. On the other hand, when the initial electron is located at M point (Fig. 4(b)), the transition probability shown in solid arrow is much higher than that shown in broken arrow because of the lack of electron state 2′. In this manner, the total number of probable transition paths was varied by the initial electron state, indicating that IITRs are strongly affected by the band index and the wave vector of initial electrons. In addition to the number of transition paths, the IITR is also affected by the momentum transfer (q) since smaller q leads to higher transition rate, as expressed in Eqs. (2a) and (2b). In the calculation, it was

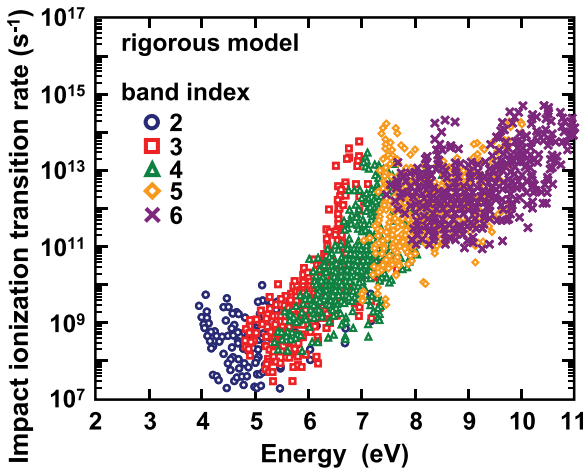

FIG. 3. Calculated impact ionization transition rate as a function of energy by rigorous model. Symbols correspond to conduction band indexes of initial electron.

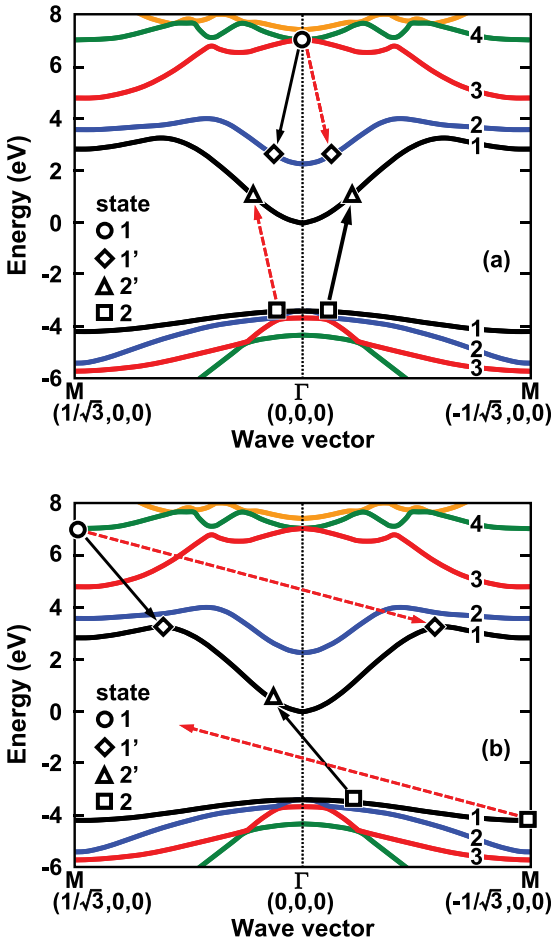

FIG. 4. Impact ionization processes for initial electrons located at (a) Γ and (b) M points. Circles correspond to electrons for state 1, squares for state 2, diamonds for state 1′, and triangles for state 2′. Arrows indicate direction of transition path.

confirmed that the initial electron located near Γ point in band index of 3, 4, or 5 showed extremely high transition rate of all electrons with energies below 8 eV in the BZ.

Figure 5 shows calculated IITRs as a function of electron energy using (a) proposed and (b) conventional models. IITRs increased with electron energy for both models. However, IITRs by the proposed model showed spreading by three orders of magnitude in accordance with the band index in the energy range from 6.5 to 8 eV. As an example, IITRs by the proposed model at 6.9 eV showed 1.3×10^{10}, 2.8×10^{12}, and 1.5×10^{11} s^{-1} for band indexes 2, 3, and 4, respectively. Meanwhile, the IITR calculated by the conventional model at 6.9 eV was 7.4×10^{11} s^{-1}, indicating that the conventional model underestimated IITRs for band index 3 and overestimated for band indexes 2 and 4 compared to the proposed model. In contrast, both models exhibited almost the same IITR values in the energy range below 6 eV and above 8.5 eV. This implies that the dependence of the band index is not significant in lower and higher energy regions.

An impact ionization coefficient of electron was calculated by a full band Monte Carlo simulation to confirm the validity of considering the band index. The calculation procedure of electron transport was the same as reported by Fischetti and Laux.[32] Rectangular cells in the BZ were

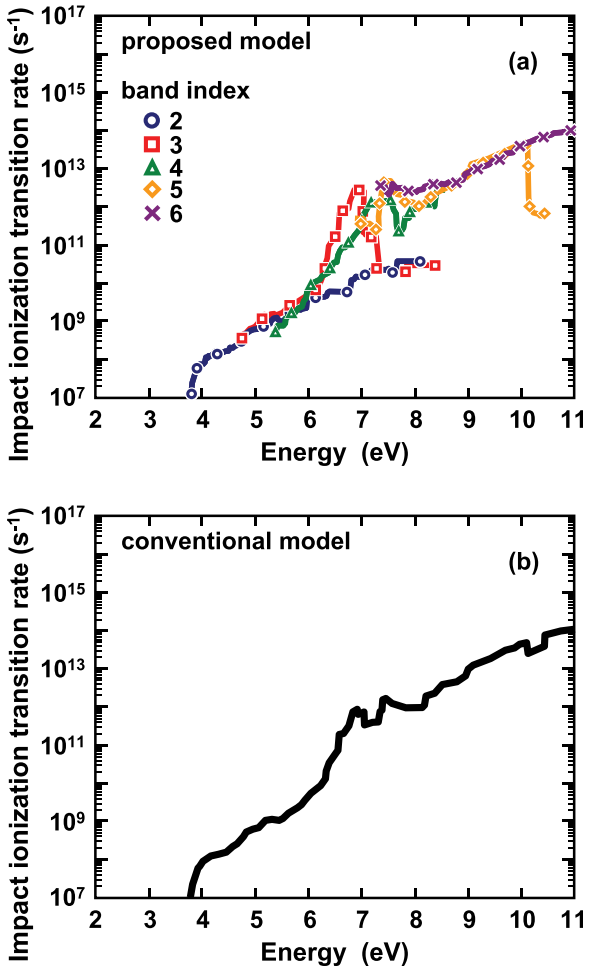

FIG. 5. Calculated impact ionization transition rate as a function of electron energy using (a) proposed and (b) conventional models. Each symbol corresponds to band index.

assumed to store physical parameters such as electron energy, group velocity, density of state, and scattering rate. For the rectangular cell, $(\Delta k_x, \Delta k_y, \Delta k_z) = 1/40(1/3, 1/\sqrt{3}, 1/2)$ was used, where the subscripts x, y, and z indicate the directions along Γ-M, Γ-K, and Γ-A in the BZ, respectively. Scattering mechanisms considered were acoustic phonon, polar and non-polar optical phonon, piezoelectric, and ionized impurity scatterings.[8,33] An impact ionization coefficient of hole was not calculated due to the majority carriers of electron in the calculation ($n = 1 \times 10^{17}\,cm^{-3}$).

Figure 6 shows the calculated impact ionization coefficient as a function of inverse electric field for three models. The electric field was applied along Γ-M direction and varied from 2 to 6 MV/cm. The impact ionization coefficient calculated by the rigorous model is in good agreement with the calculated[10] and experimental[34] results. The conventional model showed 5–15 times higher impact ionization coefficients than those by the rigorous model for the whole electric fields, while the overestimation was significantly reduced using the proposed model. Thus, it is concluded that the proposed model gives much closer ionization coefficient to that by the rigorous model. Overestimated results by the conventional model are mainly due to the contribution of electrons with an electron energy ranging from 6.5 to 8 eV, where

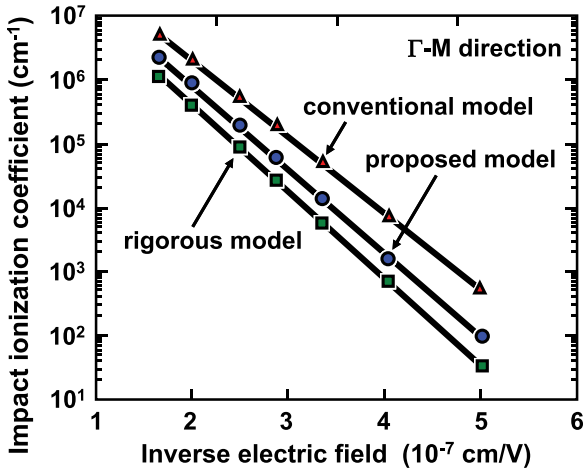

FIG. 6. Calculated impact ionization coefficient as a function of inverse electric field. Circle, triangle, and square symbols indicate ionization coefficients calculated by using proposed, conventional, and rigorous models, respectively. Electric fields from 2 to 6 MV/cm were applied along Γ-M direction.

impact ionization is governed by high values in DOS from the band index 4.

Computation time for the calculation of ionization coefficients was compared between models. The proposed model and the conventional one required 42 h to simulate 1000 particles for a time period of 500 ps at an electric field of 4 MV/cm using Intel i7-2600 CPU (3.4 GHz). On the other hand, the rigorous model demanded more than 10 times longer computation time (575 h) for the similar calculation, indicating that the rigorous model is not realistic for large-scale calculation, such as 2-dimentional device simulation.

IV. DEVICE SIMULATION IN AlGaN/GaN HEMTs

The calculation of breakdown characteristics in AlGaN/GaN HEMTs was performed based on a full band Monte Carlo device simulation incorporating IITRs by the proposed model. A schematic cross section of the simulated AlGaN/GaN HEMT is shown in Fig. 7. The structure consists of a 25 nm-thick undoped AlGaN barrier layer with Al content of 0.25, and a 250 nm-thick undoped GaN channel layer. The source-to-gate distance, gate length, and gate-to-drain distance (L_{gd}) were assumed to be 1, 1, and 3 μm, respectively.

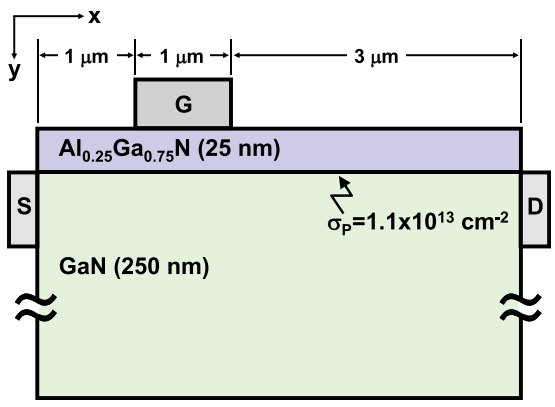

FIG. 7. Schematic cross section of AlGaN/GaN HEMT simulated in this work.

For simplicity, source and drain ohmic contacts were placed directly on the channel layer. A positive polarization charge of $1.1 \times 10^{13}\,cm^{-2}$ was assumed at AlGaN/GaN interface as reported in Ref. 14. Boltzmann transport equation was solved self-consistently using an ensemble Monte Carlo algorithm coupled with two-dimensional Poisson equation. The band structure of wurtzite AlGaN was calculated using GaN and AlN (Ref. 35) pseudopotential parameters with considering the virtual crystal approximation.[36] The grid spacings of Δx and Δy were 10 and 1 nm, respectively. The Dirichlet condition was assumed for boundary conditions of ohmic and Schottky contacts, while the Neumann condition was for other surfaces. The electric field in the device was adjusted every 1 fs. An ensemble of 10 000 particles was launched as initial conditions. The lattice temperature was 300 K.

Figure 8(a) shows static drain current-voltage characteristics calculated by the proposed model up to a drain voltage of 50 V. The maximum drain current was 600 mA/mm at a gate voltage (V_{gs}) of 1 V. The threshold voltage was −4.5 V estimated by linear extrapolation of transfer characteristics. At a drain voltage of 50 V, no impact ionization process occurred even at $V_{gs} = 1$ V. Figure 8(b) compares calculated drain current-voltage characteristics under the pinched-off condition ($V_{gs} = -5.5$ V) between proposed and conventional models.

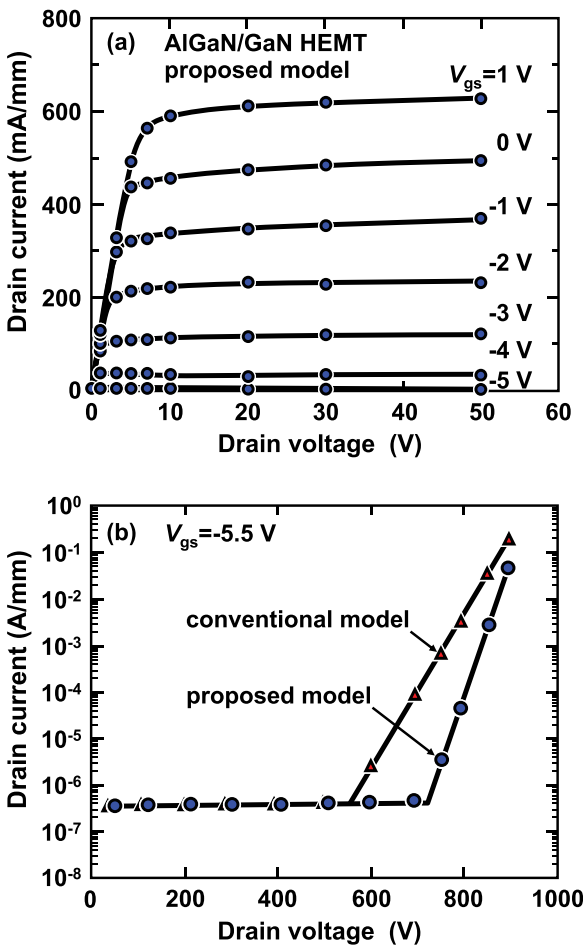

FIG. 8. Calculated results of (a) static drain current-voltage characteristics and (b) breakdown characteristics. Circles and triangles correspond to characteristics calculated by proposed and conventional models, respectively.

The V_{br} values calculated by proposed and conventional models were 720 and 550 V, respectively, indicating that the proposed model showed 30% higher V_{br} than that by the conventional model. The lower V_{br} calculated by the conventional model is consistent with the overestimated impact ionization coefficient as shown in Fig. 6. Since the proposed model indicates more accurate impact ionization coefficients than those of the conventional model, as shown in Fig. 6, the proposed model is expected to give a breakdown voltage closer to that by the rigorous model. The averaged breakdown electric field, defined as V_{br}/L_{gd}, calculated by the present model is found to be 2.4 MV/cm, which is much higher than the predicted value of 1.6 MV/cm simulated by the conventional model by Ando *et al.*[15] The breakdown field (2.4 MV/cm) is also higher than the experimental values,[16–20] suggesting that the breakdown voltage in AlGaN/GaN HEMTs would be further increased when the breakdown voltage is determined more predominantly by impact ionization than by gate or substrate leakage current.[37,38]

V. CONCLUSION

A model for calculating IITR in wurtzite GaN has been developed for use in breakdown voltage simulations. The characteristic feature of the model is to calculate energy-dependent IITR with taking a conduction band index into account. Depending on the band index, the IITR values calculated by the proposed model showed spreading by three orders of magnitude in the electron energy range from 6.5 to 8 eV, while this spreading was totally disregarded in the conventional model. An impact ionization coefficient was calculated based on a full band Monte Carlo simulation which incorporated IITRs by the proposed model. At an electric field of 2 MV/cm, the impact ionization coefficient calculated by the conventional model was overestimated by 15 times compared to that by the rigorous model, while the overestimation was significantly reduced by using the proposed model. Calculation of breakdown characteristics for AlGaN/GaN HEMTs demonstrated that the proposed model resulted in a higher breakdown voltage by about 30% than that by the conventional model.

ACKNOWLEDGMENTS

This work was performed as a part of the project named "Development of Nitride-based Semiconductor Crystal Substrate and Epitaxial Growth Technology" by NEDO.

[1]K. Kasahara, H. Miyamoto, Y. Ando, Y. Okamoto, T. Nakayama, and M. Kuzuhara, Tech. Dig. – Int. Electron Devices Meet. **2002**, 677.
[2]Y. F. Wu, A. Saxler, M. Moore, R. P. Smith, S. Sheppard, P. M. Chavarkar, T. Wisleder, U. K. Mishra, and P. Parikh, IEEE Electron Device Lett. **25**, 117 (2004).
[3]F. Lecourt, N. Ketteniss, H. Behmenburg, N. Defrance, V. Hoel, M. Eickelkamp, A. Vescan, C. Giesen, M. Heuken, and J. C. D. Jaeger, IEEE Electron Device Lett. **32**, 1537 (2011).
[4]M. Higashiwaki, T. Mimura, and T. Matsui, Appl. Phys. Express **1**, 021103 (2008).
[5]D. S. Lee, J. W. Chung, H. Wang, X. Gao, S. Guo, P. Fay, and T. Palacios, IEEE Electron Device Lett. **32**, 755 (2011).
[6]K. Shinohara, D. Regan, A. Corrion, D. Brown, S. Burnham, P. J. Willadsen, I. A. Rodriguez, M. Cunningham, C. Butler, A. Schmitz,

S. Kim, B. Holden, D. Chang, V. Lee, A. Ohoka, P. M. Asbeck, and M. Micovic, Tech. Dig. – Int. Electron Devices Meet. **2011**, 19.1.1.
[7]J. Kolník, İ. H. Oğuzman, K. F. Brennan, R. Wang, P. P. Ruden, and Y. Wang, J. Appl. Phys. **78**, 1033 (1995).
[8]S. Yamakawa, S. Aboud, M. Saraniti, and S. M. Goodnick, J. Comput. Electron. **2**, 481 (2003).
[9]V. A. Dmitriev, K. G. Irvine, C. H. Carter, Jr., N. I. Kuznetsov, and E. V. Kalinina, Appl. Phys. Lett. **68**, 229 (1996).
[10]J. Kolník, İ. H. Oğuzman, K. F. Brennan, R. Wang, and P. P. Ruden, J. Appl. Phys. **81**, 726 (1997).
[11]E. Bellotti and F. Bertazzi, J. Appl. Phys. **111**, 103711 (2012).
[12]Y. Kamakura, H. Mizuno, M. Yamaji, M. Morifuji, K. Taniguchi, and C. Hamaguchi, J. Appl. Phys. **75**, 3500 (1994).
[13]K. Yeom, J. M. Hinckley, and J. Singh, J. Appl. Phys. **80**, 6773 (1996).
[14]S. Karmalkar and U. K. Mishra, IEEE Trans. Electron Devices **48**, 1515 (2001).
[15]Y. Ando, W. Contrata, N. Samoto, H. Miyamoto, K. Matsunaga, M. Kuzuhara, K. Kunihiro, K. Kasahara, T. Nakayama, Y. Takahashi, N. Hayama, and Y. Ohno, IEEE Trans. Electron Devices **47**, 1965 (2000).
[16]P. Srivastava, J. Das, D. Visalli, M. V. Hove, P. E. Malinowski, D. Marcon, S. Lenci, K. Geens, K. Cheng, M. Leys, S. Decoutere, R. P. Mertens, and G. Borghs, IEEE Electron Device Lett. **32**, 30 (2011).
[17]H. S. Lee, D. Piedra, M. Sun, X. Gao, S. Guo, and T. Palacios, IEEE Electron Device Lett. **33**, 982 (2012).
[18]S. L. Selvaraj, A. Watanabe, A. Wakejima, and T. Egawa, IEEE Electron Device Lett. **33**, 1375 (2012).
[19]E. B. Treidel, F. Brunner, O. Hilt, E. Cho, J. Würfl, and G. Tränkle, IEEE Trans. Electron Devices **57**, 3050 (2010).
[20]M. Sun, H. S. Lee, B. Lu, D. Piedra, and T. Palacios, Appl. Phys. Express **5**, 074202 (2012).
[21]R. Chu, Y. Zhou, J. Liu, D. Wang, K. J. Chen, and K. M. Lau, IEEE Trans. Electron Devices **52**, 438 (2005).
[22]J. Liu, Y. Zhou, J. Zhu, Y. Cai, K. M. Lau, and K. J. Chen, IEEE Trans. Electron Devices **54**, 2 (2007).
[23]J. Chelikowsky, D. J. Chadi, and M. L. Cohen, Phys. Rev. B **8**, 2786 (1973).
[24]R. Wang, P. P. Ruden, J. Kolnik, I. Oguzman and K. F. Brennan, J. Phys. Chem. Solids **58**, 913 (1997).
[25]İ. H. Oğuzman, J. Kolník, K. F. Brennan, R. Wang, T. N. Fang, and P. P. Ruden, J. Appl. Phys. **80**, 4429 (1996).
[26]B. K. Ridley, *Quantum Processes in Semiconductors*, 3rd ed. (Oxford Science Publications, 1993).
[27]N. Sano and A. Yoshii, Phys. Rev. B **45**, 4171 (1992).
[28]R. Wang, P. P. Ruden, J. Kolnik, I. Oguzman, and K. F. Brennan, Mat. Res. Soc. Symp. Proc. **395**, 601 (1996).
[29]J. Kolnik, I. H. Oguzman, K. F. Brennan, R. Wang, and P. P. Ruden, J. Appl. Phys. **79**, 8838 (1996).
[30]M. Stobbe, R. Redmer, and W. Schattke, Phys. Rev. B **49**, 4494 (1994).
[31]M. Reigrotzki, R. Redmer, N. Fitzer, S. M. Goodnick, M. Dür, and W. Schattke, J. Appl. Phys. **86**, 4458 (1999).
[32]M. V. Fischetti and S. E. Laux, Phys. Rev. B **38**, 9721 (1988).
[33]S. Yamakawa, S. Goodnick, S. Aboud, and M. Saraniti, J. Comput. Electron. **3**, 299 (2004).
[34]R. McClintock, J. L. Pau, K. Minder, C. Bayram, P. Kung, and M. Razeghi, Appl. Phys. Lett. **90**, 141112 (2007).
[35]D. Fritsch, H. Schmidt, and M. Grundmann, Phys. Rev. B **67**, 235205 (2003).
[36]M. Goano, E. Bellotti, E. Ghillino, C. Garetto, G. Ghione, and K. F. Brennan, J. Appl. Phys. **88**, 6476 (2000).
[37]Q. Jiang, C. Liu, Y. Lu, and K. J. Chen, IEEE Electron Device Lett. **34**, 357 (2013).
[38]S. Arulkumaran, V. K. X. Lin, S. B. Dolmanan, G. I. Ng, S. Vicknesh, J. P. Y. Tan, S. L. Teo, M. K. Kumar, and S. Tripathy, in Proceedings of DRC, University Park, TX, 18-20 June 2012.